Agro Bali : Agricultural Journal
Vol. 9 No. 2: 490-502, July 2026
e-ISSN 2655-853X
https://doi.org/10.37637/ab.v9i2.2766

Optimizing Land-Use Scenarios for Water-Resource Sustainability in the Upper Kampar Watershed, Indonesia

Firman Hidayat[1], Agung Primatara Marwan[2♥]
[1]Forestry Study Program, Faculty of Forestry, Muhammadiyah University of West Sumatra, Padang, Indonesia
[2]Food Crops Production Technology, Plant Cultivation Department, Politeknik Pertanian Negeri Payakumbuh, Lima Puluh Kota, Indonesia
♥Corresponding author email: agung.pm12@gmail.com

Article history: submitted: April 25, 2026; accepted: July 29, 2026; available online: August 13, 2026

Abstract. Soil erosion in the Upper Kampar Watershed threatens reservoir storage and downstream water reliability. This study compared four land-use scenarios using the Universal Soil Loss Equation and the Soil Conservation Service Curve Number method across 100 land units. Existing land use produced 142.70 $t.ha^{-1}.yr^{-1}$ of soil loss, well above the tolerable value of 39.62 $t.ha^{-1}.yr^{-1}$. Meeting the minimum forest-cover rule lowered erosion by 31.95% but did not reach the threshold. Strip cropping reduced erosion to 32.90 $t.ha^{-1}.yr^{-1}$, whereas rehabilitation of mapped protected areas yielded 36.15 $t.ha^{-1}.yr^{-1}$ and the lowest Q_{max}/Q_{min} ratio (28.38). Discharge records supported directional checking, but independent event-scale validation was unavailable. The results support protected-area rehabilitation as a zoning framework, combined with soil-conservation practices on cultivated slopes and field monitoring of sediment and river flow.

Keywords: curve number; land-use planning; runoff; soil conservation; soil erosion; watershed management

1. Introduction

Soil erosion removes fertile topsoil, weakens agricultural production, and transfers sediment to rivers and reservoirs (Montanarella et al., 2016; Nearing et al., 2017). The problem is particularly acute in humid tropical watersheds, where intense rainfall interacts with steep slopes and rapid land-cover change. Global assessments show that land-use change can markedly increase water-driven soil erosion, while recent erosivity studies indicate that rainfall variability adds further uncertainty to future risk (Borrelli et al., 2017; Borrelli et al., n.d.; Fenta et al., 2024; Panagos et al., 2017). Soil-loss tolerance is therefore not only an agronomic benchmark; it is also relevant to reservoir operation and water security (Di Stefano et al., 2023).

The Upper Kampar Watershed in West Sumatra drains toward the Koto Panjang reservoir system. During the study period, forest conversion and expansion of mixed gardens, dryland farming, and settlements reduced continuous vegetation cover on erosion-prone terrain. The spatial data used in this study indicated that the resulting watershed condition was associated with high predicted soil loss and increasingly variable river flow. Comparable responses have been reported in other tropical basins, where conversion of forest to agriculture increases rapid runoff and reduces dry-season flow support (Di Stefano et al., 2023; Markum & Rahman, 2024).

Empirical models remain useful in data-limited watersheds because they can translate available rainfall, soil, topographic, and land-cover data into comparable management indicators. The Universal Soil Loss Equation (USLE) is widely used to estimate long-term sheet and rill erosion, although its empirical structure and sensitivity to input quality are well documented (Alewell et al., 2019; Benavidez et al., 2018). The Soil Conservation Service Curve Number (SCS-CN) method provides a simple representation of direct runoff response. Used together, the two models can show whether a land-use option improves soil retention and flow regulation at the same time. They do not, however, replace event-scale calibration or process-based simulation.

Previous studies often examine historical land-cover change, erosion, or runoff separately. Scenario studies also tend

e-ISSN 2655-853X
https://doi.org/10.37637/ab.v9i2.2766

to compare generic conservation alternatives without testing how statutory forest-cover requirements, field-level conservation, and protected-area rehabilitation alter the ranking of management priorities when soil loss and flow stability are assessed together. The unresolved point is whether the scenario that minimizes predicted erosion also provides the strongest regulation of maximum and minimum flow.

To examine this issue, four scenarios were compared: existing land use (S1), rehabilitation to meet the minimum forest-cover requirement (S2), S2 combined with strip cropping on mixed agricultural land (S3), and rehabilitation of mapped protected forest areas under spatial-planning principles (S4). Scientifically, the analysis tests whether soil retention and flow regulation indicators produce the same scenario ranking. In practical terms, it compares policy-based and field-management options using one land-unit database. The objectives were to quantify soil loss relative to the tolerable threshold, compare scenario-specific runoff indicators, examine the robustness of the ranking to bounded output perturbations, and identify a management option that balances biophysical performance with watershed-scale implementation. It was expected that S3 would produce the lowest erosion, whereas the larger forest allocation in S4 would provide the strongest flow regulation.

2. Materials and Methods

2.1 Study Area

The research was conducted from August 2021 to March 2022 in the Upper Kampar Watershed, Bukik Barisan Subdistrict, Lima Puluh Kota Regency, West Sumatra, Indonesia. The mapped study area covered 28,535.49 ha and included the Baruah Gunuang area and adjoining upstream Kampar drainage. Terrain ranges from flat valley floors to slopes exceeding 40%. Ultisols are dominant, followed by Inceptisols; both occur under forest, mixed gardens, shrubland, cropland, rice fields, settlements, and other land uses. Figure 1 places the study area within the regional drainage network. The GIS watershed boundary was used as the spatial reference for all overlays and area calculations.

2.2 Data Sources and Sampling

Primary and secondary data are summarized in Table 1. Four Landsat ETM+ scenes with 30-m spatial resolution represented land cover in 2005, 2010, 2015, and 2020. Daily rainfall records for 2005–2020 were obtained for the Maek and Pangkalan stations through the Sicincin office of the Indonesian Agency for Meteorology, Climatology and Geophysics. Daily and monthly discharge records for 2008–2020 were obtained from the Koto Panjang hydropower archive and SWS VI Agam–Kuantan. Contour, soil, topographic, geological, and forest-boundary maps were used to prepare the spatial database.

Land use, slope class, and soil order were overlaid to create 100 land units. One composite soil sample was collected from each land unit (n = 100). This design gave spatial coverage of all mapped combinations but did not provide within-unit replication. Soil texture was measured by the pipette method, permeability by a constant-head permeameter, and organic carbon by the Walkley–Black method. These properties were used to derive soil erodibility. Field checks were used to confirm major land-cover classes, although the available field records did not include a probability-based accuracy sample or a confusion matrix.

 e-ISSN 2655-853X
https://doi.org/10.37637/ab.v9i2.2766

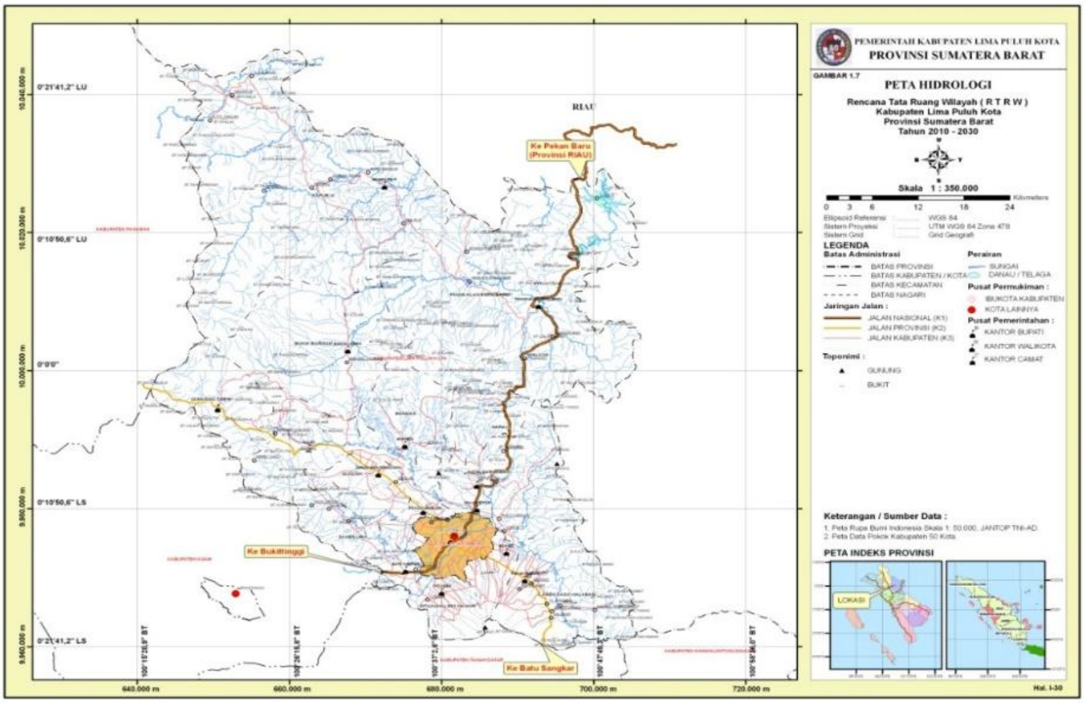

Figure 1. Regional hydrological setting of Lima Puluh Kota Regency and the Upper Kampar study-area context. The map is used for regional orientation; it does not replace the land-unit boundary data used in the spatial analysis. Source: Lima Puluh Kota Regency spatial-plan hydrology map (2010–2030).

Table 1. Data used in the erosion and runoff scenario analysis.

Class	Data	Coverage or source	Use
Primary	Soil physical and chemical properties	100 land-unit samples	Derivation of soil erodibility and support for tolerable soil-loss estimation
Primary	Land-cover condition and field checks	Field observations and Landsat ETM+ interpretation	Land-cover assignment and verification of major classes
Secondary	Landsat ETM+ imagery	2005, 2010, 2015, and 2020; 30 m	Historical land-cover mapping and scenario baseline
Secondary	Topography and soils	1:50,000 contour, slope, soil, geology, and forest-boundary maps	Land-unit construction; LS and hydrologic-soil-group assignment
Secondary	Rainfall	Daily records, 2005–2020; Maek and Pangkalan stations	Rainfall erosivity and runoff input
Secondary	River discharge	Daily and monthly records, 2008–2020	Directional plausibility checking of flow response

Note. ETM+ = Enhanced Thematic Mapper Plus; LS = combined slope-length and slope-steepness factor.

2.3 Spatial Processing

Landsat scenes were processed in ERDAS using maximum-likelihood supervised classification. Land-cover maps were then overlaid in ArcView with soil order and five slope classes (0–8%, >8–15%, >15–25%, >25–40%, and >40%). This overlay generated the 100 land units used for parameter assignment and soil sampling. The workflow is summarized in Figure 2. Classification uncertainty was considered during interpretation because the available classification records did not include the reference samples needed to calculate an area-adjusted accuracy estimate. Current good practice would require independent reference samples and area-weighted accuracy measures (Stehman & Foody, 2019).

e-ISSN 2655-853X
https://doi.org/10.37637/ab.v9i2.2766

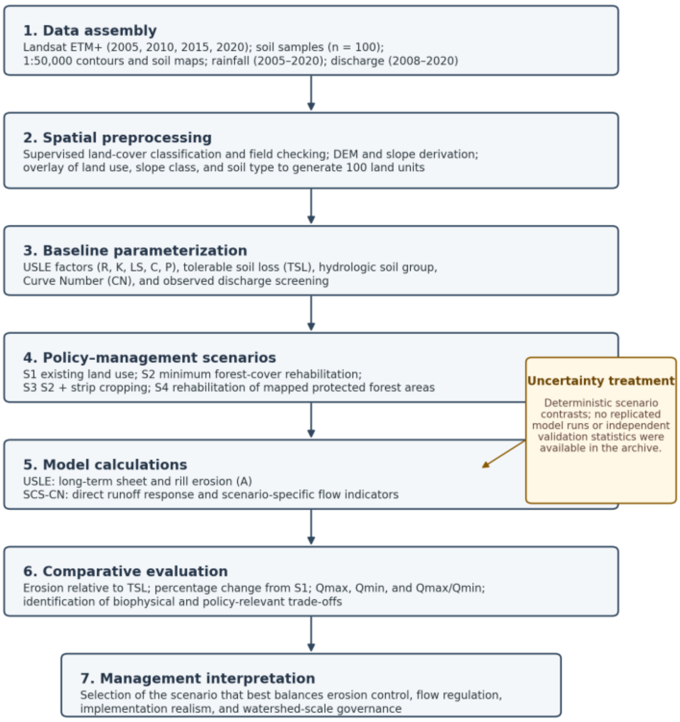

Figure 2. Analytical workflow for assembling the land-unit database, parameterizing the USLE and SCS-CN models, constructing four management scenarios, and comparing erosion and flow indicators. The uncertainty box distinguishes comparative scenario screening from formal probabilistic validation.

2.4 Land-Use Scenarios

Scenario 1 retained the 2020 land-use allocation. Scenario 2 increased forest cover from 27.97% to 39.04% of the mapped watershed, thereby satisfying the minimum 30% forest-cover requirement in Forestry Law No. 41 of 1999 (Republic of Indonesia, 1999). Scenario 3 retained the S2 land allocation and applied strip cropping to mixed agricultural land, which reduced the combined cover-management and support-practice factor. Scenario 4 followed the distinction between protected and cultivation areas in Spatial Planning Law No. 26 of 2007 and rehabilitated all mapped protected forest areas (Republic of Indonesia, 2007). Table 2 shows the land allocation and weighted CP value used for each scenario.

Table 2. Land-use allocation and cover-management/support-practice factors for the four scenarios.

Land use	S1 (ha)	S2 (ha)	S3 (ha)	S4 (ha)	CP value
Forest	7,980.96	11,141.46	11,141.46	18,108.69	0.001
Mixed gardens	12,629.32	7,598.66	7,598.66	2,309.31	0.200; 0.010 in S3
Shrubland	2,603.97	3,211.25	3,211.25	1,968.51	0.300
Cropland/moorland	2,067.22	3,330.10	3,330.10	2,906.20	0.400
Settlement	69.70	69.70	69.70	58.46	0.150
Other mapped uses	3,184.32	3,184.32	3,184.32	3,184.32	Not assigned
Total area	28,535.49	28,535.49	28,535.49	28,535.49	—
Weighted CP	0.030	0.020	0.002	0.010	—

Note. S1 = existing land use; S2 = minimum forest-cover rehabilitation; S3 = S2 plus strip cropping; S4 = protected-area rehabilitation; CP = combined cover-management and support-practice factor. “Other mapped uses” were retained in the area balance; no CP coefficient was available for these categories.

e-ISSN 2655-853X
https://doi.org/10.37637/ab.v9i2.2766

2.5 Soil-Loss Estimation

Average annual sheet and rill erosion was estimated for each land unit with the Universal Soil Loss Equation (Alewell et al., 2019; Wischmeier & Smith, 1978). The method was selected because the available database contained the rainfall, soil, topographic, land-cover, and management variables required by USLE, but not the continuous weather, crop-growth, channel, and calibration data needed for process-based models. USLE remains suitable for comparative long-term screening when its empirical scope is stated clearly (Alewell et al., 2019; Benavidez et al., 2018).

$$A = R \times K \times LS \times C \times P \quad (1)$$

In Equation 1, A is annual soil loss ($t.ha^{-1}.yr^{-1}$), R is rainfall erosivity, K is soil erodibility, LS combines slope length and steepness, C is the cover-management factor, and P is the support-practice factor. Monthly erosivity was derived with the Indonesian rainfall relationship used in the source analysis (Bols, 1978), and annual R was obtained by summing the monthly values. Soil erodibility was derived from texture, organic matter, structure, and permeability, while LS was obtained from the slope database. The raster factors were multiplied in the GIS environment. USLE does not estimate gully erosion, mass movement, sediment redeposition, or sediment delivery to the reservoir.

Tolerable soil loss (TSL) was calculated from equivalent soil depth (De), minimum soil depth (Dmin), assumed land-use life (UGT), and soil-formation rate (LPT):

$$TSL = (De - Dmin) / UGT + LPT \quad (2)$$

The resulting watershed benchmark was 39.62 $t.ha^{-1}.yr^{-1}$. Scenario outputs were compared with this threshold rather than interpreted as direct measurements of sediment yield.

2.6 Runoff Estimation

Direct runoff was estimated with the Soil Conservation Service Curve Number method (SCS-CN; U.S. Department of Agriculture Soil Conservation Service, 1972). This approach was chosen because the available inputs supported a consistent comparison among land-use scenarios, whereas a calibrated SWAT or HEC-HMS application would have required event-scale rainfall–discharge pairs and additional channel parameters that were not available. For rainfall P greater than the initial abstraction, runoff depth Q was calculated as follows:

$$Q = (P - 0.2S)^2 / (P + 0.8S) \quad (3)$$

$$S = (25{,}400 / CN) - 254 \quad (4)$$

In Equations 3 and 4, P and Q are in millimetres, S is the maximum potential retention, and CN is the curve number. CN was assigned based on land cover, treatment, hydrologic conditions, antecedent moisture, and hydrologic soil group. Group A has the highest infiltration capacity and Group D the lowest. The available discharge series was used to check whether the direction of simulated change was hydrologically plausible, but it was not sufficient for independent event-scale calibration and validation. Consequently, Qmax, Qmin, and Qmax/Qmin are treated as comparative scenario indicators rather than fully validated forecasts. Scenario 3 retained the same land-cover allocation, hydrologic soil groups, and antecedent-moisture assumptions as Scenario 2. The strip-cropping intervention was therefore represented in USLE through the combined cover-management and support-practice factor, whereas the archived SCS-CN calculation retained the Scenario 2 CN values. USDA NRCS guidance shows that agricultural treatment and hydrologic conditions can justify different CN values, including lower values for contouring and residue cover (U.S. Department of Agriculture Natural Resources Conservation Service, 2004). However, the study archive did not contain locally verified CN adjustments for strip cropping. A separate reduction was not imposed because doing so would introduce an uncalibrated hydrologic effect and could double-count benefits already represented in the erosion model. This conservative assumption may understate

e-ISSN 2655-853X
https://doi.org/10.37637/ab.v9i2.2766

the runoff benefit of Scenario 3 and should be tested with event-scale rainfall-runoff data in future applications.

2.7 Comparative and Uncertainty Analysis

Each scenario was a single deterministic realization. Replicated model runs, probability distributions for input factors, and independent validation events were unavailable; therefore, p-values, confidence intervals, and inferential effect sizes would not be statistically defensible. The analysis instead reported absolute differences, percentage change from S1, the ratio of predicted erosion to TSL, and the margin above or below TSL as deterministic measures of scenario effect. Descriptive calculations and scenario comparisons were completed in Microsoft Excel, while the spatial overlays were processed in ERDAS and ArcView.

Table 3. Hydrologic soil groups used in the SCS-CN parameterization.

Group	General soil characteristics	Minimum infiltration (mm.h−1)
A	Deep sand, deep loess, or well-aggregated silt	8–12
B	Shallow loess or sandy loam	4–8
C	Clay loam, shallow sandy loam, low-organic-matter soil, or high-clay soil	1–4
D	Swelling soil, heavy clay, plastic clay, or selected saline soil	0–1

Note. SCS-CN = Soil Conservation Service Curve Number. The ranges reproduce the classification used in the source analysis.

A transparent threshold-robustness screening perturbed each reported erosion output by −20%, +10%, and +20%. These levels were selected as simple decision-screening values rather than as probability-based uncertainty bounds. The 10% perturbation represents a modest departure from the reported output, whereas 20% provides a stronger stress test against the tolerable soil-loss threshold. The choice was based on analyst judgement and one-at-a-time screening practice, not on estimated error distributions for the model inputs. Such screening can be useful when full probabilistic ranges are unavailable, provided that it is distinguished clearly from formal global sensitivity and uncertainty analysis (Pianosi et al., 2016; Saltelli et al., 2019). For the flow indicator, a conservative interval was calculated by decreasing Qmax and increasing Qmin by 10% for the lower bound, and increasing Qmax and decreasing Qmin by 10% for the upper bound. These bounds are not confidence intervals. They show whether the scenario ranking and threshold classification remain stable under bounded output variation. Rainfall erosivity, satellite classification, DEM quality, CN assignment, and the lack of within-unit soil replication were considered the principal uncertainty sources (Bezak et al., 2022; Fenta et al., 2024; Polidori & El Hage, 2020).

3. Results and Discussion

3.1 Erosion Response to the Four Scenarios

The first research objective was to determine whether the scenarios reduced soil loss below the tolerable threshold. Table 4 shows that S1 produced 142.70 t.ha−1.yr−1, or 3.60 times the TSL. Increasing forest cover to the statutory minimum in S2 reduced erosion by 31.95%, but the predicted rate remained 57.49 t.ha−1.yr−1 above the threshold. S3 produced the lowest erosion (32.90 t.ha−1.yr−1), a reduction of 76.94% from S1 and a margin of 6.72 t.ha−1.yr−1 below TSL. S4 also met the threshold at 36.15 t.ha−1.yr−1, 74.67% below S1 and 3.47 t.ha−1.yr−1 below TSL. Thus, the erosion results were consistent with the expectation that strip cropping in S3 would provide the strongest soil-loss control.

e-ISSN 2655-853X
https://doi.org/10.37637/ab.v9i2.2766

Table 4. Predicted erosion, relative change, and position against the tolerable soil-loss threshold.

Scenario	Erosion (t.ha−1.yr−1)	Change from S1 (%)	Erosion/TSL	Margin from TSL (t.ha−1.yr−1)	Status
S1	142.70	0.00	3.60	+103.08	Above TSL
S2	97.11	−31.95	2.45	+57.49	Above TSL
S3	32.90	−76.94	0.83	−6.72	Below TSL
S4	36.15	−74.67	0.91	−3.47	Below TSL

Note. TSL = tolerable soil loss (39.62 t.ha−1.yr−1). Positive margins indicate erosion above TSL; negative margins indicate erosion below TSL.

3.2 Flow-Regulation Response

The second objective was to compare flow regulation. Table 5 shows that S4 had the lowest Qmax (54.76 $m^3.s^{-1}$), the highest Qmin (1.94 $m^3.s^{-1}$), and the lowest Qmax/Qmin ratio (28.38). Relative to S1, Qmax declined by 20.82%, Qmin increased by 36.62%, and the flow ratio declined by 42.26%. S2 and S3 produced the same hydrological outputs because they had identical land allocation and CN parameterization in the runoff analysis. Strip cropping changed the USLE CP factor in S3 but was not represented as a separate CN adjustment. Thus, the flow results supported the expectation that S4 would provide the strongest regulation of maximum and minimum flow.

Table 5. Maximum flow, minimum flow, and river-regime ratio under each scenario.

Scenario	Qmax ($m^3.s^{-1}$)	Qmin ($m^3.s^{-1}$)	Qmax/Qmin	Ratio change from S1 (%)
S1	69.16	1.42	49.15	0.00
S2	64.62	1.52	42.50	−13.53
S3	64.62	1.52	42.50	−13.53
S4	54.76	1.94	28.38	−42.26

Note. Qmax = maximum discharge; Qmin = minimum discharge. Ratios were calculated from unrounded discharge values; Qmax and Qmin are displayed to two decimal places.

3.3 Robustness of the Ranking

The screening analysis addressed the third objective by testing whether the main conclusions were sensitive to bounded output changes. Table 6 shows that S3 remained just below TSL after a 20% upward perturbation (39.48 t.ha−1.yr−1). S4 crossed the threshold after a 10% increase (39.77 t.ha−1.yr−1), which indicates a narrower safety margin. The conservative Qmax/Qmin bounds did not reverse the hydrological ranking: the upper bound for S4 (34.69) remained below the lower bounds for S2 and S3 (34.77) and below the lower bound for S1 (40.21). Figure 3 summarizes the contrasting erosion and flow responses.

Table 6. Deterministic robustness screening for erosion and the Qmax/Qmin ratio.

Scenario	Erosion −20%	Erosion +10%	Erosion +20%	TSL response	Ratio lower bound	Ratio upper bound
S1	114.16	156.97	171.24	Above all tested increases	40.21	60.07
S2	77.69	106.82	116.53	Above all tested increases	34.77	51.94
S3	26.32	36.19	39.48	Below at +20%	34.77	51.94
S4	28.92	39.77	43.38	Crosses at +10%	23.22	34.69

Note. Erosion is expressed in t.ha−1.yr−1. Ratio bounds apply opposite ±10% perturbations to Qmax and Qmin. These values are screening bounds, not confidence intervals.

e-ISSN 2655-853X
https://doi.org/10.37637/ab.v9i2.2766

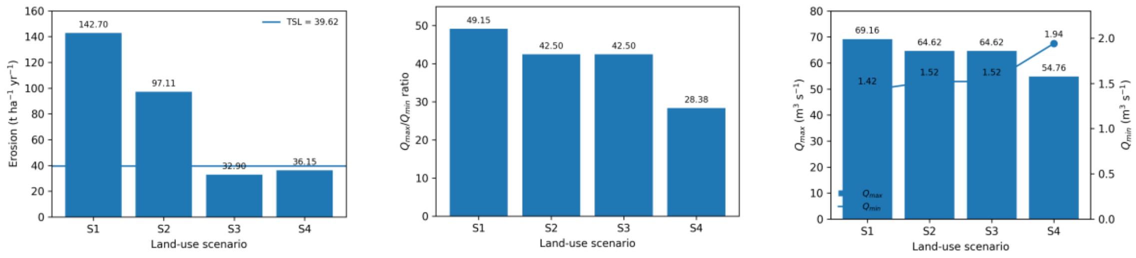

(a) Erosion and TSL *(b) Qmax/Qmin ratio* *(c) Maximum and minimum flow*

Figure 3. Scenario outputs used to compare (a) predicted soil loss with the tolerable threshold, (b) flow variability, and (c) maximum and minimum discharge. Values reproduce Tables 4 and 5.

3.4 Interpretation of the Forest-Cover Scenario

3.4.1 Why Forest Cover Alone Did Not Meet the Soil-Loss Threshold

The decline from S1 to S2 confirms that forest rehabilitation reduces exposure of the soil surface and lowers the spatial extent of high-CP land. The reduction was substantial but insufficient because cultivated and shrub-covered slopes remained in the landscape, and their management factors continued to dominate predicted soil loss. Similar reviews of USLE applications show that forest cover is effective. Still, the final erosion response depends on the location of that cover, slope, soil erodibility, and management of the remaining agricultural land (Alewell et al., 2019; Benavidez et al., 2018). The result, therefore, supports a combined strategy rather than reliance on a watershed-wide percentage target alone.

3.4.2 Why Strip Cropping Produced the Lowest Erosion

Scenario 3 reduced the weighted CP factor from 0.020 in Scenario 2 to 0.002 while retaining the same land allocation. This change explains why Scenario 3 achieved the lowest erosion, even though Scenarios 2 and 3 had identical runoff outputs in the archived SCS-CN analysis. Strip cropping interrupts downslope flow paths, increases surface roughness, and places more protective cover across the slope, thereby reducing the transport capacity of shallow runoff. Meta-analyses and field studies show that vegetative strips, contour-aligned barriers, and continuous cover can reduce both runoff and soil loss, although the magnitude varies with slope, rainfall, soil, and maintenance quality (Prosdocimi et al., 2016; Rajbanshi et al., 2023). The robustness check also shows that Scenario 3 had the stronger threshold margin, although its +20% value was only 0.14 t.ha−1.yr−1 below TSL. This narrow margin still warrants field verification.

3.4.3 Why Protected-Area Rehabilitation Improved Flow Regulation

Scenario 4 allocated 18,108.69 ha to forest, substantially more than the other scenarios, and concentrated rehabilitation in mapped protected areas. The lower Qmax, higher Qmin, and smaller Qmax/Qmin ratio are consistent with several interacting hydrological pathways. Canopy and litter intercept rainfall and delay its delivery to the soil surface; roots, biological pores, and improved aggregate stability can increase infiltration and reduce rapid overland flow; and infiltrated water can be stored temporarily in the unsaturated zone, move laterally through the soil, or contribute to groundwater recharge before returning to the channel. These processes delay storm runoff and can support low flows where infiltration remains functional. Evidence from regenerating tropical forests shows improved infiltration and reduced overland flow. At the same time, broader studies caution that the net effect of tree cover on recharge and streamflow varies with climate, geology, soil properties, species, and stand age (Ilstedt et al., 2016; van Meerveld et al., 2021; van Dijke et al., 2022). In the Upper Kampar analysis, these processes were not measured directly; they provide a mechanistic interpretation of the modeled pattern rather than independent validation.

e-ISSN 2655-853X
https://doi.org/10.37637/ab.v9i2.2766

The difference between S3 and S4 is therefore a genuine management trade-off. S3 is the erosion-control optimum represented by the current model, whereas S4 is the hydrological and zoning optimum. Treating S4 as universally superior would overstate the evidence because its erosion margin was less robust. A defensible policy package would use S4 to define the protected-area framework, then apply S3-type practices on cultivated slopes that remain outside rehabilitated forest. This combined interpretation preserves the original purpose of the study while avoiding the unsupported claim that one scenario dominates every criterion.

3.4.4 Transferability, Model Validation, and Implementation

The analytical sequence can be transferred to other tropical watersheds that have land-cover, soil, slope, rainfall, and discharge data. Still, the numerical coefficients should not be transferred without local checking. CN values, soil erodibility, rainfall erosivity, and tolerable soil loss are site-dependent. Recent scenario work likewise shows that land-use rankings can change with model structure and local environmental constraints (Qiao et al., 2024; Tian et al., 2021). The absence of independent event-scale calibration and validation limits the accuracy of the absolute runoff values because CN, initial abstraction, and rainfall timing were not optimized against an independent set of observed events. It also prevents the reporting of standard model-performance statistics (Moriasi et al., 2015). Nevertheless, the relative ranking remains useful as a screening result because all scenarios were evaluated with the same rainfall, soil, topographic framework, model equations, and baseline parameter rules; only the land-use and management assumptions changed. This common-baseline design reduces, but does not remove, systematic bias. The results should therefore be interpreted as comparative evidence for prioritization, not as operational forecasts of discharge.

Implementation also depends on land tenure, farmer incentives, maintenance costs, and institutional coordination. Forest rehabilitation can restrict short-term access to cultivated land, while strip cropping requires repeated field-level management. Restoration programs are more durable when local communities participate in design and benefit sharing (Erbaugh et al., 2020). A practical sequence would begin with updated land-cover and tenure mapping, followed by prioritization of land units that exceed TSL and are hydrologically connected to the main drainage network. Protected and riparian slopes could then be rehabilitated through assisted natural regeneration or locally appropriate planting, while retained mixed gardens and cropland would receive contour-aligned strips, permanent ground cover, or equivalent conservation measures. Watershed managers, local governments, village institutions, and the reservoir operator should agree on responsibilities, incentives, maintenance schedules, and a shared monitoring protocol before large-scale implementation.

4. Limitations and Future Directions

First, USLE estimates long-term sheet and rill erosion; it does not simulate gullies, landslides, channel erosion, sediment redeposition, or sediment delivery. The outputs should not be interpreted as measured reservoir sedimentation. A future study should combine plot measurements, suspended-sediment monitoring, and a process-based or sediment-delivery model.

Second, the land-cover classification was based on 30-m Landsat scenes and field checking. Still, the archived files did not contain an independent probability sample, a confusion matrix, or an area-adjusted confidence interval. Mixed pixels and spectral similarity among shrubland, mixed gardens, and cropland may therefore affect area and CP assignments. Future mapping should follow rigorous accuracy-assessment practice with independent reference samples (Stehman & Foody, 2019).

Third, rainfall came from two stations and was summarized from historical daily records. The network may not capture short-duration convective storms or orographic gradients across steep terrain. Rainfall erosivity is sensitive to temporal resolution, and recent satellite–gauge and radar products could improve spatial and intra-annual representation (Bezak et al., 2022; Fenta et al., 2024; Matthews et al., 2025).

Fourth, DEM scale and processing influence slope length and steepness. Vertical error and resolution mismatch may propagate into LS and runoff pathways (Polidori & El Hage, 2020). The 100 soil samples provided broad spatial coverage, but no within-unit replication; local variation in texture, organic carbon, and permeability was therefore not quantified.

Fifth, the SCS-CN outputs were checked directionally against available discharge records, but were not independently calibrated and validated at the event scale. This limits confidence in the absolute Qmax and Qmin values and means that standard predictive-performance measures cannot be reported. The ranking is still appropriate for preliminary comparison because all scenarios share the same model structure and baseline forcing; however, land-cover-specific parameter errors could still alter the magnitude, and possibly the ordering, of scenario effects. The screening perturbations in Table 6 are not probability-based uncertainty intervals. Future work should retain event rainfall and discharge pairs, calibrate CN or a process-based hydrological model, and report performance metrics on an independent validation period (Moriasi et al., 2015).

Finally, the scenarios assume complete policy implementation and do not incorporate climate change, landholder response, costs, or temporal transitions during rehabilitation. Future analysis should couple climate projections with land-use trajectories, sediment monitoring, and socio-economic optimization. The global evidence that land-use and rainfall erosivity may change together makes this extension particularly important (Borrellia et al., 2020; Fenta et al., 2024).

5. Conclusion

The scenario comparison answers the study objectives without treating one option as superior on every criterion. Existing land use produced erosion far above the tolerable threshold. Meeting the minimum forest-cover requirement reduced erosion but was not sufficient. Forest rehabilitation combined with strip cropping produced the lowest erosion (32.90 $t.ha^{-1}.yr^{-1}$), whereas rehabilitation of mapped protected areas produced the strongest flow regulation and reduced the Qmax/Qmin ratio to 28.38. The recommended strategy is therefore a combined one: use protected-area rehabilitation as the watershed zoning framework and require contour-aligned strip cropping, permanent cover, or equivalent conservation measures on cultivated slopes that remain outside rehabilitated forest.

For implementation, watershed managers and local governments should first update land-cover, slope-risk, and tenure maps; identify land units above TSL that are directly connected to streams; and agree on a phased rehabilitation and conservation schedule with village institutions and landholders. Monitoring should prioritize land-cover change, plot-scale soil loss, suspended sediment, rainfall, Qmax, Qmin, and dry-season flow at representative subcatchments. CP and CN assignments should be reviewed as field data accumulate, and the policy package should include maintenance responsibilities, farmer incentives, and periodic cost-benefit assessment. Because the hydrological model was not independently validated at the event scale and Scenario 4 had a narrow erosion margin, the proposed strategy should be implemented adaptively rather than treated as a fixed prediction.

Declaration of Generative AI and AI-Assisted Technologies

During manuscript revision, the authors used ChatGPT for language editing and document

e-ISSN 2655-853X
https://doi.org/10.37637/ab.v9i2.2766

organization. All numerical results, citations, interpretations, and final wording were reviewed by the authors, who take full responsibility for the content of the manuscript.

Author Contributions

Author 1: Conceptualization, methodology, investigation, data curation, and formal analysis. Author 2: Writing—original draft, validation, formal analysis, investigation, and writing—review and editing.

Declaration of Competing Interest

The authors declare that they have no known competing financial interests or personal relationships that could have influenced the work reported in this paper.

Acknowledgments

The authors thank the Forestry Study Program, Faculty of Forestry, Universitas Muhammadiyah Sumatera Barat, for institutional support.

References

Alewell, C., Borrelli, P., Meusburger, K., & Panagos, P. (2019). Using the USLE: Chances, challenges and limitations of soil erosion modelling. *International Soil and Water Conservation Research*, *7*(3), 203–225. https://doi.org/10.1016/j.iswcr.2019.05.004

Benavidez, R., Jackson, B., Maxwell, D., & Norton, K. P. (2018). A review of the (Revised) Universal Soil Loss Equation ((R)USLE): With a view to increasing its global applicability and improving soil loss estimates. *Hydrology and Earth System Sciences*, *22*(11), 6059–6086. https://doi.org/10.5194/hess-22-6059-2018

Bezak, N., Borrelli, P., & Panagos, P. (2022). Exploring the possible role of satellite-based rainfall data in estimating inter- and intra-annual global rainfall erosivity. *Hydrology and Earth System Sciences*, *26*(7), 1907–1924. https://doi.org/10.5194/hess-26-1907-2022

Bols, P. L. (1978). *The iso-erodent map of Java and Madura*.

Borrelli, P., Robinson, D. A., Fleischer, L. R., Lugato, E., Ballabio, C., Alewell, C., Meusburger, K., Modugno, S., Schütt, B., Ferro, V., Bagarello, V., Van Oost, K., Montanarella, L., & Panagos, P. (2017). An assessment of the global impact of 21st century land use change on soil erosion. *Nature Communications*, *8*(1), 2013. https://doi.org/10.1038/s41467-017-02142-7

Borrelli, P., Robinson, D. A., Panagos D □, P., Lugato, E., Yang, J. E., Alewell, C., Wuepper, D., Montanarella, L., & Ballabio, C. (n.d.). *Land use and climate change impacts on global soil erosion by water (2015-2070)*. https://doi.org/10.1073/pnas.2001403117/-/DCSupplemental

Borrellia, P., Robinson, D. A., Panagos, P., Lugato, E., Yang, J. E., Wuepper, D., Montanarella, L., & Ballabio, C. (2020). Land use and climate change impacts on global soil erosion by water (2015-2070) _ Enhanced Reader. *PNAS*, *117*, 21994–22001.

Di Stefano, C., Nicosia, A., Pampalone, V., & Ferro, V. (2023). Soil loss tolerance in the context of the European Green Deal. *Heliyon*, *9*(1). https://doi.org/10.1016/j.heliyon.2023.e12869

Erbaugh, J. T., Pradhan, N., Adams, J., Oldekop, J. A., Agrawal, A., Brockington, D., Pritchard, R., & Chhatre, A. (2020). Global forest restoration and the importance of prioritizing local communities. *Nature Ecology & Evolution*, *4*(11), 1472–1476. https://doi.org/10.1038/s41559-020-01282-2

Fenta, A. A., Tsunekawa, A., Haregeweyn, N., Yasuda, H., Tsubo, M., Borrelli, P., Kawai, T., Belay, A. S., Ebabu, K., Berihun, M. L., Sultan, D., Setargie, T. A., Elnashar, A., Arshad, A., & Panagos, P. (2024). An integrated modeling approach for estimating monthly global rainfall erosivity. *Scientific Reports*, *14*(1), 8167. https://doi.org/10.1038/s41598-024-59019-1

Ilstedt, U., Bargués Tobella, A., Bazié, H. R., Bayala, J., Verbeeten, E., Nyberg, G., Sanou, J., Benegas, L., Murdiyarso, D., Laudon, H., Sheil, D., & Malmer, A. (2016). Intermediate tree cover can maximize groundwater recharge in the seasonally dry tropics. *Scientific Reports*, *6*(1), 21930. https://doi.org/10.1038/srep21930

Markum, & Rahman, F. A. (2024). Surface runoff in varying forest cover types in Jangkok Watershed, Lombok Island, Indonesia.

e-ISSN 2655-853X
https://doi.org/10.37637/ab.v9i2.2766

Biodiversitas, *25*(2), 753–761. https://doi.org/10.13057/biodiv/d250235

Matthews, F., Borrelli, P., Panagos, P., & Bezak, N. (2025). Dynamic assessment of rainfall erosivity in Europe: Evaluation of EURADCLIM ground-radar data. *Hydrology and Earth System Sciences*, *29*, 5299–5313. https://doi.org/10.5194/hess-29-5299-2025

Montanarella, L., Pennock, D. J., McKenzie, N., Badraoui, M., Chude, V., Baptista Costa, I. D. S., Mamo, T., Yemefack, M., Aulang, M. S., Yagi, K., Hong, S. Y., Vijarnsorn, P., Zhang, G. L., Arrouays, D., Black, H., Krasilnikov, P., Sobocká, J., Alegre, J., Henriquez, C. R., … Vargas, R. (2016). World's soils are under threat. *SOIL*, *2*(1), 79–82. https://doi.org/10.5194/soil-2-79-2016

Moriasi, D. N., Gitau, M. W., Pai, N., & Daggupati, P. (2015). Hydrologic and water quality models: Performance measures and evaluation criteria. *Transactions of the ASABE*, *58*(6), 1763–1785. https://doi.org/10.13031/trans.58.10715

Nearing, M. A., Xie, Y., Liu, B., & Ye, Y. (2017). Natural and anthropogenic rates of soil erosion. *International Soil and Water Conservation Research*, *5*(2), 77–84. https://doi.org/10.1016/j.iswcr.2017.04.001

Panagos, P., Borrelli, P., Meusburger, K., Yu, B., Klik, A., Lim, K. J., Yang, J. E., Ni, J., Miao, C., Chattopadhyay, N., Sadeghi, S. H., Hazbavi, Z., Zabihi, M., Larionov, G. A., Krasnov, S. F., Gorobets, A. V, Levi, Y., Erpul, G., Birkel, C., … Ballabio, C. (2017). Global rainfall erosivity assessment based on high-temporal resolution rainfall records. *Scientific Reports*, *7*(1), 4175. https://doi.org/10.1038/s41598-017-04282-8

Pianosi, F., Beven, K., Freer, J., Hall, J. W., Rougier, J., Stephenson, D. B., & Wagener, T. (2016). Sensitivity analysis of environmental models: A systematic review with practical workflow. *Environmental Modelling & Software*, *79*, 214–232. https://doi.org/10.1016/j.envsoft.2016.02.008

Polidori, L., & El Hage, M. (2020). Digital elevation model quality assessment methods: A critical review. *Remote Sensing*, *12*(21), 3522. https://doi.org/10.3390/rs12213522

Prosdocimi, M., Cerdà, A., & Tarolli, P. (2016). Soil water erosion on Mediterranean vineyards: A review. *Catena*, *141*, 1–21. https://doi.org/10.1016/j.catena.2016.02.010

Qiao, X., Li, Z., Lin, J., Wang, H., Zheng, S., & Yang, S. (2024). Assessing current and future soil erosion under changing land use based on InVEST and FLUS models in the Yihe River Basin, North China. *International Soil and Water Conservation Research*, *12*(2), 298–312. https://doi.org/10.1016/j.iswcr.2023.07.001

Rajbanshi, J., Das, S., & Paul, R. (2023). Quantification of the effects of conservation practices on surface runoff and soil erosion in croplands and their trade-off: A meta-analysis. *Science of the Total Environment*, *864*, 161015. https://doi.org/10.1016/j.scitotenv.2022.161015

Republic of Indonesia. (1999). *Law of the Republic of Indonesia Number 41 of 1999 concerning forestry*.

Republic of Indonesia. (2007). *Law of the Republic of Indonesia Number 26 of 2007 concerning spatial planning*.

Saltelli, A., Aleksankina, K., Becker, W., Fennell, P., Ferretti, F., Holst, N., Li, S., & Wu, Q. (2019). Why so many published sensitivity analyses are false: A systematic review of sensitivity analysis practices. *Environmental Modelling & Software*, *114*, 29–39. https://doi.org/10.1016/j.envsoft.2019.01.012

Stehman, S. V, & Foody, G. M. (2019). Key issues in rigorous accuracy assessment of land cover products. *Remote Sensing of Environment*, *231*, 111199. https://doi.org/10.1016/j.rse.2019.05.018

Tian, P., Zhu, Z., Yue, Q., He, Y., Zhang, Z., Hao, F., Guo, W., Chen, L., & Liu, M. (2021). Soil erosion assessment by RUSLE with improved P factor and its validation: Case study on mountainous and hilly areas of Hubei Province, China. *International Soil and Water Conservation Research*, *9*(3), 433–444. https://doi.org/10.1016/j.iswcr.2021.04.007

U.S. Department of Agriculture Natural Resources Conservation Service. (2004). *Hydrologic soil-cover complexes* (National

e-ISSN 2655-853X
https://doi.org/10.37637/ab.v9i2.2766

Engineering Handbook, Part 630, Chapter 9).

U.S. Department of Agriculture Soil Conservation Service. (1972). *National engineering handbook, Section 4: Hydrology*.

van Dijke, A. J., Herold, M., Mallick, K., Benedict, I., Machwitz, M., Schlerf, M., Pranindita, A., Theeuwen, J. J. E., Bastin, J.-F., & Teuling, A. J. (2022). Shifts in regional water availability due to global tree restoration. *Nature Geoscience*, *15*, 363–368. https://doi.org/10.1038/s41561-022-00935-0

van Meerveld, H. J., Jones, J. P. G., Ghimire, C. P., Zwartendijk, B. W., Lahitiana, J., Ravelona, M., & Mulligan, M. (2021). Forest regeneration can positively contribute to local hydrological ecosystem services: Implications for forest landscape restoration. *Journal of Applied Ecology*, *58*(4), 755–765. https://doi.org/10.1111/1365-2664.13836

Wischmeier, W. H., & Smith, D. D. (1978). *Predicting rainfall erosion losses: A guide to conservation planning* (Agriculture Handbook No. 537)